Benzyl ether : a dynamic covalent motif for designing a trans-ether based covalent adaptable network (CAN)

Kumar, Pawan; Gupta, Vatsalya; Majumdar, Soumabrata; Patwal, Rahul; Das, Debabrota et al

Check for updates

Benzyl ether: a dynamic covalent motif for designing a trans-ether based covalent adaptable network (CAN)†

Pawan Kumar, [ID] [a] Vatsalya Gupta, [ID] [a] Soumabrata Majumdar, [ID] [c] Rahul Patwal, [ID] [a] Debabrota Das, [ID] [b] Prabin Kumar Ashish [ID] [b] and Ramkrishna Sarkar [ID] *[a]

This report introduces benzyl ether-based trans-etherification as a new robust chemistry for designing CANs. The dynamic ether exchange and its dissociative nature are demonstrated using small molecule model studies. Along with reprocessability, the CAN also exhibits efficient stress relaxation. This study expands the library of chemistries for the development of CAN.

The covalent adaptable network (CAN) is a unique class of chemically crosslinked polymeric material that possesses thermoset-like mechanical robustness under operating conditions while exhibiting malleability and reprocessability under certain conditions, like thermoplastics. The reprocessability of CANs is attributed to the presence of functional groups within the network that undergo bond exchange reactions upon activation by a stimulus such as heat or light.[1–6] Various dynamic covalent motifs such as urethane, urea, ester, imine, boronic ester, acetal, thioether, disulfide, and reactions such as Diels–Alder, have been integrated into polymer networks to achieve their properties.[7–15]

Designing chemistry that imparts both robustness and dynamicity to the resulting CANs has become a major area of research in recent years, with a focus on tailoring their properties. To this end, we introduce benzyl ether-based trans-ether exchange as a robust dynamic chemistry to design CAN (Fig. 1). Surprisingly, to the best of our knowledge, the ether bond, which is known to endow the chemical inertness and robustness of polymeric materials, has not been explored in the CANs. While exchangeable ether linkages have yet to be explored in CANs, their congeners, silyl ester chemistries, have recently been introduced. Guan and coworkers reported

thermally robust CANs based on silyl ether exchange chemistry.[16,17] Unlike several other previously reported CANs, the silyl ether-based CANs showed an appreciable thermal stability up to 427 °C ($T_{d,5\%}$). McCarthy and coworkers reported dynamic siloxane chemistry, which enabled the robustness and self-healability of the networks.[18] More recently, numerous reports on silyl ether-based CANs have been reported in the literature.[19–21] Subsequently, transthioetherification has been reported for CAN design. Du Prez's group demonstrated a photoinduced thioether-sulfonium salt-based network, which shows CAN properties.[22,23] Kalow and coworkers reported the PDMS vitrimer utilizing conjugate addition–elimination of thiols.[24] Additionally, other studies have also reported the use of thioether chemistry in the development of CANs.[25]

Inspired by the ether linkages' robustness and versatility, we explore this linkage, specifically benzyl ether, towards the development of CAN. Contrary to most others, benzylic ethers show a significantly higher reactivity towards substitution reactions. Ramakrishnan and coworkers have previously reported the polymerization of benzyl ethers *via* transetherification.[26] Inspired by this approach, we conceived the idea of exploring transetherification on benzylic ethers as a new dynamic covalent chemistry (DCC) for the design of CANs (Fig. 1).

[a] Polymer Chemistry Group, Department of Chemistry, Indian Institute of Technology Kanpur, Kanpur, Uttar Pradesh, 208016, India. E-mail: ramkrishna@iitk.ac.in

[b] Department of Civil Engineering, Indian Institute of Technology Kanpur, Kanpur, 208016, India

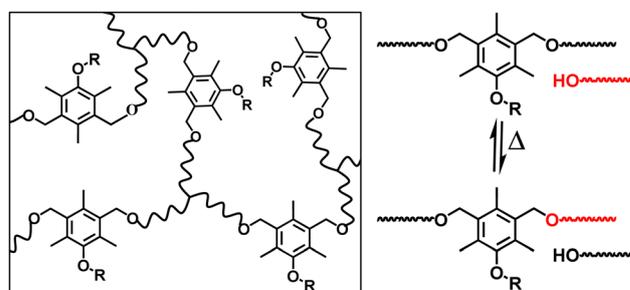*[c] Department of Physical Chemistry and Soft Matter, Wageningen University and Research, Wageningen, 6700 HB, The Netherlands*

Fig. 1 Schematic representations of the transether-based CAN (left) and dynamic ether exchange in benzyl ether (right).

In this work, we demonstrate a simple one-step method to synthesize a trans-ether based CAN using melt transetherification of a difunctional benzyl ether (**BMM-TMB**) with tri-functional alcohol, trimethylolpropane in the presence of *p*-toluene sulfonic acid (pTSA) as a catalyst. The CAN exhibited appreciable viscous flow at elevated temperatures because of transetherification-mediated bond exchange in the network. It also showed modestly high thermal robustness by virtue of having ether groups as the only functional group in the network. The malleability and reprocessability of the CAN can be readily realized through dynamic ether exchange at elevated temperatures.

In order to prepare the trans-ether-based CAN, the dibenzyl ether-bearing monomer, 1-butoxy-3,5-bis(methoxymethyl)-2,4,6-trimethylbenzene, a benzyl methyl ether (**BMM-TMB**) was first synthesized from mesitol in three steps, as shown in Scheme 1a. The synthetic details can be found in the ESI† (Fig. S1–S11).[27,28]

Prior to network synthesis, to probe the ether exchange in our monomer (**BMM-TMB**), its transetherification with 1-hexanol was carried out in the presence of pTSA at 140 °C (Scheme 1b). The ^{1}H NMR studies confirmed the formation of hexyl ether, **BBHM-TMB**, *via* transetherification (Fig. S12–S14, ESI†). However, due to the volatility of the methanol, which is formed in the course of the reaction, the reverse reaction, where the starting methyl ether (**BMM-TMB**) reforms from hexyl ether (**BBHM-TMB**), did not occur in this reversible transetherification. In order to prove the dynamic and reversible nature of the ether linkage, a more detailed study on the ether exchange kinetics was performed using **BBHM-TMB** and a less volatile alcohol, 2-(2-methoxyethoxy)ethanol (**MEE**), as the nucleophile and pTSA as the catalyst (Scheme 1c and Scheme S1, ESI†). The reactions were carried out at temperatures ranging from 110 to 140 °C. The transetherified product (**BBMEM-TMB**) showed a chemical shift of 4.56 ppm in the ^{1}H NMR spectrum, which was distinctly different from the benzylic proton of the starting **BBHM-TMB** (4.47 ppm), which helped probe the conversion

using ^{1}H NMR spectroscopy (Fig. S15, ESI†). Since **BBHM-TMB** is bifunctional in benzyl ether, the conversion was calculated based on the functional group conversion rather than the formation of the disubstituted product, **BBMEM-TMB**. A large excess of **MEE** (∼30 eq. w.r.t **BBHM-TMB**) was used for the reactions, resulting in pseudo-first order kinetics on **BBHM-TMB** (Fig. S16, ESI†). The rate constants ranged from 0.00401 to 0.02556 s^{-1} between 110 and 140 °C. The activation energy for the reaction from the Arrhenius plot (Fig. 1d) was found to be 77.07 kJ mol^{-1}. It was also shown that when a lower equivalent of **MEE** was used under similar conditions, equilibrium was reached in nearly 100 minutes at 130 °C (Fig. S17, ESI†). Thus, these studies revealed the exchangeability and dynamic nature of the benzyl ether. It is important to note that, in this exchange reaction, despite **BBHM-TMB** containing two types of ethers, namely benzyl, and phenyl, the ether exchange was not observed in the phenyl ether center, confirming the importance of the benzyl ether for the ether's exchangeability.

Furthermore, to investigate the mechanism of the benzylic ether exchange reaction, *i.e.*, the associative or dissociative nature of the exchange, dibenzyl ether (**BBHM-TMB**) was heated along with phthalic anhydride in the presence of pTSA (Scheme 2a). The formation of the phthalate ester, as probed by NMR and ESI-MS, revealed an operating dissociative mechanism. 1-Hexanol, formed as a result of benzylic ether dissociation, converted the reactive anhydride to the corresponding ester, and benzylic ether segments transformed to the corresponding alcohol (Fig. S18–S20, ESI†). Besides, multiple control studies were also conducted. The control reaction between phthalic anhydride and 1-hexanol within similar conditions also showed phthalate ester formation (Fig. S22, ESI†). No reaction was observed when **BBHM-TMB** and phthalic anhydride were heated at 140 °C in the absence of pTSA, showing the inertness of **BBHM-TMB** (Fig. S21, ESI†). It is important to mention here that phthalic anhydride remains unchanged when heated separately solely with the same catalyst under similar conditions, also confirming its inertness towards the employed reaction conditions (Fig. S23, ESI†).

Additional model studies were conducted to gain further insights into this exchange (Scheme 2b). The **BMM-TMB** monomer was treated with pentamethylbenzene (**PMB**) in the presence of pTSA as a catalyst at 140 °C. The single aromatic proton in **PMB** enabled easy tracking of the reaction, making it a suitable model reactant for our study. The NMR (^{1}H and ^{13}C) and ESI-MS studies
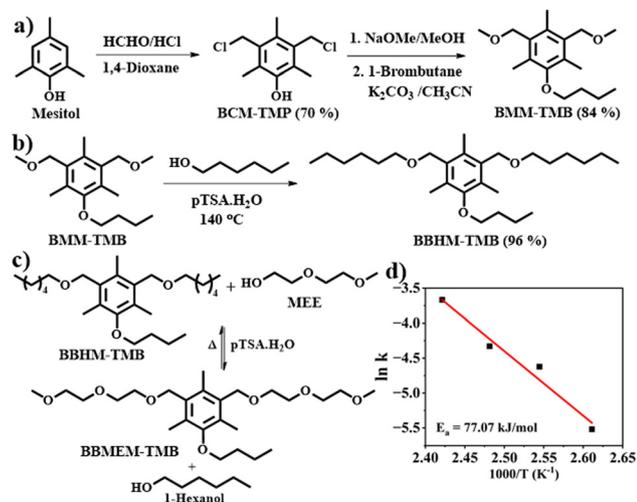
Scheme 1 (a) Synthesis scheme of the dibenzyl ether bearing monomer, **BMM-TMB**, starting from mesitol. (b) The scheme showing ether exchange in the **BMM-TMB**. (c) Exchange reaction between **BBHM-TMB**, and **MEE**. (d) Determination of the activation energy using the Arrhenius plot.
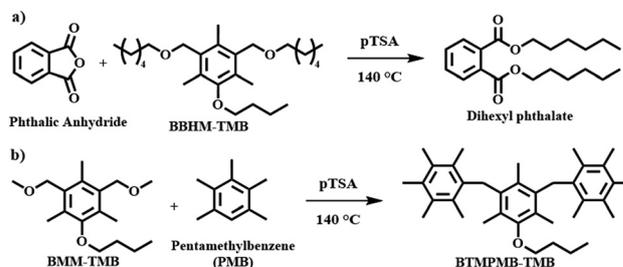

Scheme 2 (a) Model studies demonstrating the dissociative nature of the ether exchange. (b) Model studies of **BMM-TMB** and **PMB** showing the formation of **PMB-TMB**.

revealed the formation of the **PMB**-bearing product, **PMB-TMB** (Fig. S24–S26, ESI†). This suggests that the *in situ* generated benzylic carbocation underwent Friedel–Crafts type electrophilic substitution reaction with **PMB**. In the literature, the transetherification is also proposed to proceed through the formation of a benzylic carbocation.[27,28]

To explore the polymerization ability of **BMM-TMB** *via* transetherification, its polymerization with a diol, triethylene glycol, was carried out in the presence of pTSA H$_2$O (Scheme 3a). **BMM-TMB** is a safe choice as the completely substituted aromatic ring disallowed the above-mentioned undesired electrophilic aromatic substitution reaction. The polymerization resulted in a linear polyether, **MESTEG**, with benzyl ether linkages. The formation of the linear polymer was confirmed by ^{1}H NMR spectroscopy (Fig. S27, ESI†). The molecular weight of **MESTEG** was determined using gel permeation chromatography (GPC). The GPC analysis revealed a number average molecular weight of 40 800 g mol^{-1}, with a polydispersity index (Đ) of 1.90 (Fig. S28, ESI†).

Upon successful demonstration of the benzyl ether's exchange and its polymerization ability, the trans-ether based CAN (network) was prepared using similar melt transetherification of **BMM-TMB** with tri-functional alcohol, trimethylolpropane using 5 mol% pTSA (Scheme 3b). The equimolarity of alcohol and ether was maintained. Thus, complete conversion would ensure no unreacted free alcohols except those arising from network defects. The polymerization was carried out at 145 °C for 12 h with constant nitrogen purging, ensuring the removal of the methanol by-product and facilitating network formation. The gel fraction of the network was measured to be 89.4% in dichloromethane and 90.2% in THF. FT-IR analysis revealed the disappearance of characteristic peaks in **BMM-TMB** associated with the methyl ether (Ar–CH$_2$–O–**CH$_3$**) at 2823 cm^{-1} and 1190 cm^{-1} and hydroxyl stretch in trimethylolpropane (at 3228 cm^{-1}), suggesting network formation (Fig. S29–S30, ESI†).

The thermal characteristics of the linear polymer and network were examined by thermogravimetric analysis (TGA) and differential scanning calorimetry (DSC). Due to the robustness of the ether linkage, good thermal stability was anticipated. TGA studies indeed demonstrated notable thermal stability. TGA analysis revealed minimal weight loss up to 200 °C, with a 5% weight loss temperature ($T_{d,5\%}$) observed to be 263 °C and 292 °C for the linear polymer and network, respectively (Fig. 2a
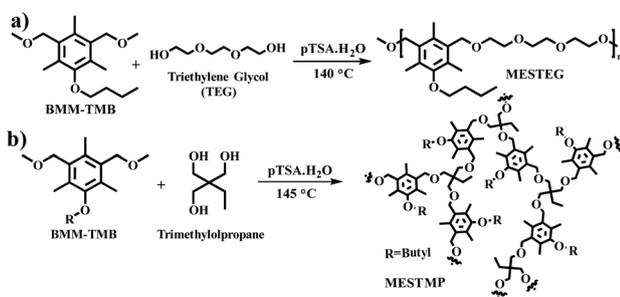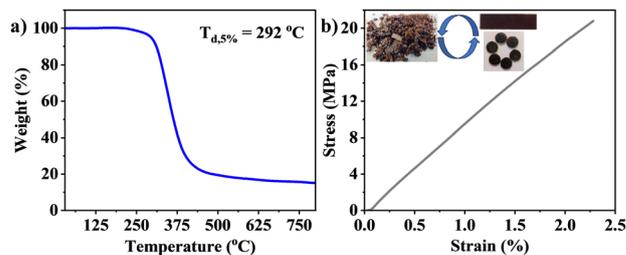
Fig. 2 (a) TGA profile of the network (**MESTMP**) recorded at a heating rate of 10 deg min^{-1}. (b) Tensile plot of **MESTMP**. The inset shows the reprocessability of the **MESTMP**.

and Fig. S31a, ESI†). The $T_{d,5\%}$ of our current CAN, **MESTMP**, is notably high (Fig. S32, ESI†). This significantly expands the feasible temperature range for practical material processing and applications. Furthermore, the isothermal TGA study of the network performed at two different temperatures, *i.e.*, 185 °C and 215 °C, also revealed good thermal stability (Fig. S33, ESI†). Furthermore, DSC analysis revealed a glass transition temperature (T_g) of −29 °C and 92 °C for the linear polymer and network, respectively (Fig. S31b and S34, ESI†). Additionally, the CANs also exhibited good solvent stability, as evidenced by their stability tests in various chemicals and solvents (Fig. S35, S36 and Table S1, ESI†).

The ability to reshape and reprocess at elevated temperatures is a pivotal characteristic of CANs. This is attributed to the dynamic bond exchange within the network. Our network possesses dynamic benzylic ether linkage, so topological rearrangement and processability are anticipated. The dynamic nature of the synthesized network was demonstrated through compression molding of the grounded material. This process involved heating at 170 °C under a pressure of 10 MPa for 60 minutes, resulting in disk and rectangular-shaped materials (Fig. 2b inset). No significant difference was observed between the FT-IR spectra of the pristine and reprocessed networks, indicating no substantial change in the material's chemical structure due to reprocessing (Fig. S37, ESI†). The tensile properties of these processed films were then determined (Fig. 2b). The Young's modulus, elongation at break, and ultimate tensile strength of the CAN were found to be 934.5 MPa, 2.30%, and 20.80 MPa, respectively.

To explore the dynamic behavior of CANs, stress-relaxation experiments were conducted on compression-molded samples at temperatures ranging from 140 °C to 170 °C under a 5% step strain (Fig. 3a). The relaxation modulus $G(t)$ was normalized at t = 1 second. Since the material is composed of dynamic benzyl ether linkages, the network showed an effective relaxation of the imposed stress at elevated temperatures. A faster relaxation was observed at higher temperatures, whereas a slower relaxation was observed at relatively lower temperatures due to the slower rate of exchange at lower temperatures. The characteristic relaxation times (τ) were obtained using a stretched mono-exponential fit to the obtained data (eqn (S1), ESI†). At 170 °C, which is the processing temperature of the material, the network showed a faster relaxation with a characteristic relaxation time (τ) of 187 s, which further increased to 393 s, 701 s, and 1794 s at 160 °C,

Scheme 3 Synthesis scheme for the preparation of (a) linear polyether, **MESTEG**, and (b) trans-ether-based network **MESTMP** using the melt transetherification route.
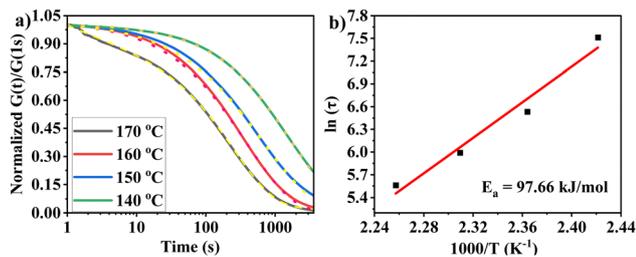
Fig. 3 (a) Stress-relaxation profile of the benzyl ether network, **MESTMP** at 170 °C, 160 °C, 150 °C and 140 °C. (b) Activation energy plot obtained using the Arrhenius equation.

150 °C, and 140 °C, respectively. Finally, the apparent activation energy was obtained using the Arrhenius equation (eqn (S2), ESI†), which was found to be 97.66 kJ mol⁻¹ (Fig. 3b).

Finally, with the aim of a suitable end-of-life solution, degradation studies of the polymer and network were examined. Polymer degradation and chemical recycling is one of the useful strategies for waste minimization.[29–31] The linear polyether (**MESTEG**) could be completely degraded upon treatment with excess alcohol (1-hexanol) at 140 °C in the presence of 5 mol% added pTSA to obtain the **BBHM-TMB** in 79% yield. Degradation of the network was also performed with excess 1-hexanol at 140 °C. The network was fully degraded and completely dissolved. However, recovery of the monomer was a challenging task. The transetherification of the ether linkage with excess 1-hexanol at elevated temperatures resulted in their disintegration *via* the cleaving of the polymer backbone and de-crosslinking of the network, respectively (Fig. S38–S39, ESI†).

In conclusion, our study showcases the transetherification of benzyl ether as a novel chemistry for developing thermoset-like CAN. To the best of our knowledge, this is the first study wherein the transetherification chemistry has been utilized to develop CAN. The model studies demonstrated the dynamic exchangeability and dissociative nature of the benzylic ether group. The CAN exhibited excellent thermal properties, reprocessability, and efficient stress relaxation. Overall, this study introduces new avenues for developing CANs. Ether linkages are known to impart robustness, and we anticipate that incorporating dynamic ether chemistry will lead to significant advancements in developing robust, dynamic materials.

Data availability

Data supporting this article have been included in the ESI.†

Conflicts of interest

The authors declare no conflicts of interest.

Notes and references

1 C. J. Kloxin, *et al.*, *Macromolecules*, 2010, **43**, 2643–2653.
2 W. Zou, *et al.*, *Adv. Mater.*, 2017, **29**, 1606100.
3 G. M. Scheutz, *et al.*, *J. Am. Chem. Soc.*, 2019, **141**, 16181–16196.
4 C. Bowman, *et al.*, *Polym. Chem.*, 2020, **11**, 5295–5296.
5 S. J. Rowan, *et al.*, *Angew. Chem., Int. Ed.*, 2002, **14**, 898–952.
6 W. Denissen, *et al.*, *Chem. Sci.*, 2016, **7**, 30–38.
7 Y. X. Lu, *et al.*, *J. Am. Chem. Soc.*, 2012, **134**, 8424–8427.
8 W. Denissen, *et al.*, *Adv. Funct. Mater.*, 2015, **25**, 2451–2457.
9 M. M. Obadia, *et al.*, *J. Am. Chem. Soc.*, 2015, **137**, 6078–6083.
10 O. R. Cromwell, *et al.*, *J. Am. Chem. Soc.*, 2015, **137**, 6492–6495.
11 M. Röttger, *et al.*, *Science*, 2017, **356**, 62–65.
12 L. Zhang and S. J. Rowan, *Macromolecules*, 2017, **50**, 5051–5060.
13 R. Wink, *et al.*, *Polym. Chem.*, 2023, **14**, 4294–4302.
14 R. Sarkar, *et al.*, *J. Polym. Sci.*, 2023, **61**, 1335–1347.
15 S. K. Schoustra, *et al.*, *ACS Appl. Polym. Mater.*, 2024, **6**, 79–89.
16 C. A. Tretbar, *et al.*, *J. Am. Chem. Soc.*, 2019, **141**, 16595–16599.
17 Y. Nishimura, *et al.*, *J. Am. Chem. Soc.*, 2017, **139**, 14881–14884.
18 P. Zheng and T. J. McCarthy, *J. Am. Chem. Soc.*, 2012, **134**, 2024–2027.
19 H. Fouilloux, *et al.*, *Angew. Chem., Int. Ed.*, 2022, **61**, e202113443.
20 R. Hada, *et al.*, *Macromolecules*, 2022, **55**, 5474–5484.
21 I. C. Pierce, *et al.*, *ACS Appl. Polym. Mater.*, 2024, **6**, 8697–8705.
22 N. Van Herck, *et al.*, *Angew. Chem., Int. Ed.*, 2020, **59**, 3609–3617.
23 B. Hendriks, *et al.*, *ACS Macro Lett.*, 2017, **6**, 930–934.
24 B. M. El-Zaatari, *et al.*, *Polym. Chem.*, 2020, **11**, 5339–5345.
25 D. Van Ooteghem, *et al.*, *Int. J. Sulfur Chem.*, 1973, **8**, 31–35.
26 G. C. Behera and S. Ramakrishnan, *J. Polym. Sci., Part A: Polym. Chem.*, 2004, **42**, 102–111.
27 M. Jayakannan and S. Ramakrishnan, *Chem. Commun.*, 2000, 1967–1968.
28 M. Jayakannan and S. Ramakrishnan, *Macromol. Chem. Phys.*, 2000, **201**, 759–767.
29 M. A. Alraddadi, *et al.*, *Polym. Chem.*, 2021, **12**, 5796–5802.
30 E. G. Morado, *et al.*, *Nat. Chem.*, 2023, **15**, 569–577.
31 R. L. Snyder, *et al.*, *Macromolecules*, 2018, **51**, 389–397.